ADVANCED HEALTHCARE MATERIALS
www.advhealthmat.de

Bioinspired Dopamine/Mucin Coatings Provide Lubricity, Wear Protection, and Cell-Repellent Properties for Medical Applications

*Jian Song, Theresa M. Lutz, Nora Lang, and Oliver Lieleg**

Even though medical devices have improved a lot over the past decades, there are still issues regarding their anti-biofouling properties and tribological performance, and both aspects contribute to the short- and long-term failure of these devices. Coating these devices with a biocompatible layer that reduces friction, wear, and biofouling at the same time would be a promising strategy to address these issues. Inspired by the adhesion mechanism employed by mussels, here, dopamine is made use of to immobilize lubricious mucin macromolecules onto both manufactured commercial materials and real medical devices. It is shown that purified mucins successfully adsorb onto a dopamine pre-coated substrate, and that this double-layer is stable toward mechanical challenges and storage in aqueous solutions. Moreover, the results indicate that the dopamine/mucin double-layer decreases friction (especially in the boundary lubrication regime), reduces wear damage, and provides anti-biofouling properties. The results obtained in this study show that such dopamine/mucin double-layer coatings can be powerful candidates for improving the surface properties of medical devices such as catheters, stents, and blood vessel substitutes.

1. Introduction

Medical devices such as artificial joints, catheters, stents, and blood vessel substitutes, are typically fabricated from synthetic materials and are essential for current medical therapies.[1] For those devices to fulfill their envisioned function in the human body, excellent biocompatibility, appropriate mechanical strength, low friction surfaces, as well as high resistance toward wear, corrosion and biofouling are required.[2] A main limitation of many implant materials is the cell-adhesive behavior of their surfaces, the ensuing biofouling events and the following inflammation response of the body.[3] For instance, neointimal hyperplasia occurs after the placement of metallic stents and polytetrafluoroethylene (PTFE)-based blood vessel substitutes.[4] Neointimal proliferation is induced by inflammatory reactions after the placement of the stent or blood vessel substitute followed by proliferation and migration of smooth muscle cells and production of extracellular matrix. As a possible consequence, restenosis sets in and such a closure of the luminal vessel diameter in the device can be associated with high morbidity and mortality rates.[5] Similar issues apply to other medical devices including catheters, where—in addition to eukaryotic colonization events—adhesion of bacteria to the catheter surface aggravates the risk for inflammation.[6] Moreover, if the lubricity of a medical device is not good, mechanical shear forces occurring during the implantation process can lead to the transfer of small tissue parts (or single cells) onto the device—and this will speed up the biofouling process.[7] Of course, the generation of wear by tribological stress acting on the load-bearing surface of a device can also be a direct reason for both, the short- and long-term failure of certain medical devices.[8]

To prevent those issues, coating synthetic materials with a biocompatible layer is a promising strategy.[9] One candidate for a biopolymer, which establishes coatings with anti-biofouling, lubricity and wear protection abilities, is the glycoprotein mucin. Mucins are key components of mucosal systems such as the tear fluid, saliva, or stomach mucus and have become popular due to their superior biocompatibility, excellent tribological performance, as well as anti-bacterial and anti-biofouling properties.[10] However, mucin-based coatings described in the literature are either based on passive adsorption[11] (which works well on polydimethylsiloxane (PDMS)-based surfaces but does not create stable coatings that withstand mechanical shear very well) or involve covalent coupling methods[12] (which require polymeric

Dr. J. Song, T. M. Lutz, Prof. O. Lieleg
Department of Mechanical Engineering and Munich School of Bioengineering
Technical University of Munich
85748 Garching, Germany
E-mail: oliver.lieleg@tum.de
Dr. N. Lang
Department of Pediatric Cardiology and Congenital Heart Disease, German Heart Center Munich
Technical University of Munich
80636 Munich, Germany

The ORCID identification number(s) for the author(s) of this article can be found under https://doi.org/10.1002/adhm.202000831

DOI: 10.1002/adhm.202000831

substrates that can be chemically activated). For metallic surfaces such as steel or PTFE-based materials; however, neither of those two approaches are very promising as there are no appropriate functional groups on those surfaces that were to offer anchoring points for a stable mucin attachment.[13] Yet, those materials are frequently used in biomedical applications, which calls for a different coupling strategy to generate stable mucin coatings on them.

Mussels can strongly adhere to almost any material—regardless of its surface roughness. To do so, they produce proteins rich in special tyrosine derivates called 3,4-dihydroxyphenylalanine (DOPA); DOPA molecules (as well as the chemically related neurotransmitter dopamine) belong to the group of catechols and are present at high concentrations in the tip of the mussel byssus. Catechols such as DOPA or dopamine as well as the self-polymerized variant of the latter, polydopamine, can bind to a broad range of organic and inorganic surfaces.[14] This is made possible by the ability of catechols to engage in different molecular interactions with surfaces: examples include complex formation between metal atoms of a metallic surface and the phenolic hydroxyl groups of catechols, hydrophobic interactions and/or π–π stacking, electrostatic interactions, and hydrogen bonds.[15] The same set of molecular interactions can bind other molecules to an adsorbed dopamine layer. Recently, a simple one-step coating based on dopamine was introduced to immobilize dextran onto various substrates.[16] Similarly, with the help of dopamine, polyethylene glycol (PEG, uncharged polymer),[17] polyethyleneimine (PEI, polycationic polymer),[18] and hyaluronic acid (HA, polyanionic polymer)[19] have been deposited onto different surfaces. Thus, using a similar approach might also allow for creating stable but non-covalent mucin coatings on medical devices.

We here develop dopamine/mucin coatings on materials frequently used for medical devices, that is, PDMS, PTFE, and steel substrates, using a simple dip-coating approach. We confirm the successful formation of the double-layer coatings and evaluate the lubricity, wear resistance and cell-repellent properties provided by these dopamine/mucin coatings. By performing cellular adhesion tests with real medical devices, for example, catheters, stents, and blood vessel substitutes, we demonstrate that our approach can also be applied to irregularly shaped, curved objects and as it establishes cell-repellent surfaces on those medical devices as well.

2. Results and Discussion

2.1. Generating Dopamine/Mucin Double-Layer Coatings by Sequential Adsorption

Dopamine spontaneously and firmly adsorbs onto a broad range of surfaces including glass, different metals, and polymers.[14] Here, we aim at harnessing this property by utilizing dopamine pre-coatings on different substrates to immobilize mucin glycoproteins. The idea is to conduct a two-step dip-coating procedure, where first dopamine molecules and then mucins self-assemble on the substrate surface thus forming a double-layer by sequential adsorption (**Figure 1**a). In a first step, we verify the successful formation of such a molecular double-layer by conducting QCM-D (quartz crystal microbalance with dissipation monitoring) measurements with quartz crystals carrying three different surfaces: steel, PTFE, and PDMS surfaces (see Section 4.) are chosen as model substrates as those materials are commonly used for medical devices.[20] For all three surfaces, the frequency shift (Δf) recorded in such QCM-D measurements shows a notable change when a dopamine solution is injected (Figure 1b). This frequency shift is somewhat stronger for the PDMS and steel surfaces than for the PTFE surface; in turn, the adsorption kinetics are faster for dopamine adsorption onto the PTFE substrate. After unbound dopamine is removed by rinsing with buffer, a mucin solution is injected. Also here, in all three cases, we detect a strong decrease in Δf. This indicates, that the mucin macromolecules successfully adsorb onto the pre-coated substrates, and with similar efficiencies for all three substrates.

To verify that the double-layer coatings can also be successfully generated on a macroscopic scale, we next subject cm-sized specimens of all three substrate types to a sequential dip-coating procedure (see Section 4.) and measure the contact angle of each substrate at different steps of the dip-coating process: as a bare substrate, after the first coating layer (dopamine) was applied, and after the top layer (mucin) was added to the dopamine pre-coating. For comparison, we also conduct a single-step coating with mucins, that is, without a dopamine pre-coating. As depicted in Figure 1c, both the dopamine coating and the dopamine/mucin double coating reduces the contact angles of all substrates; we find the strongest effect on the hydrophobic substrates, that is, PDMS and PTFE, but also a noticeable effect on steel. Interestingly, the contact angles obtained with a single-step mucin coating are always higher than those achieved with the other two coatings. This indicates that, whereas mucin can passively adsorb onto a wide range of surfaces, the efficiency of this adsorption process is improved when a dopamine pre-coating is used.[21] Moreover, it underscores the results we obtained with QCM-D and demonstrates that a macroscopic dopamine/mucin double coating can be easily developed on very different substrates including hydrophobic PDMS/PTFE and hydrophilic steel.

Having established that the dopamine pre-coating can immobilize mucin glycoproteins on different substrates, we next employ AFM imaging to examine the morphological quality of the coatings at the nanoscale. To obtain images with good quality, we use atomically flat mica as a substrate to carry the coating. As can be seen in Figure 1d, we do not detect any obvious defects. Moreover, with the exception of a few isolated structures in the dopamine/mucin coatings that might indicate local polydopamine or mucin fibers extending from the surface,[22] the roughness of the coating is less than 1 nm—also for the dopamine/mucin double-layers. In addition, with fluorescence microscopy using ATTO 594 labeled mucins, we detect a continuous mucin layer on the PDMS samples (Figure S1, Supporting Information), indicating good homogeneity and full surface coverage of the coatings.

Thus, we conclude that the quality of the coatings we developed in this work should be suitable to be used in further experiments. In detail, we aim at probing the lubricity, wear protection abilities, and cell repellent properties and of such dopamine-based coatings on model substrates. Moreover, we will decide if such double-layer coatings are indeed required to obtain the full set of functionalities we envision for a biomedical application. Then,

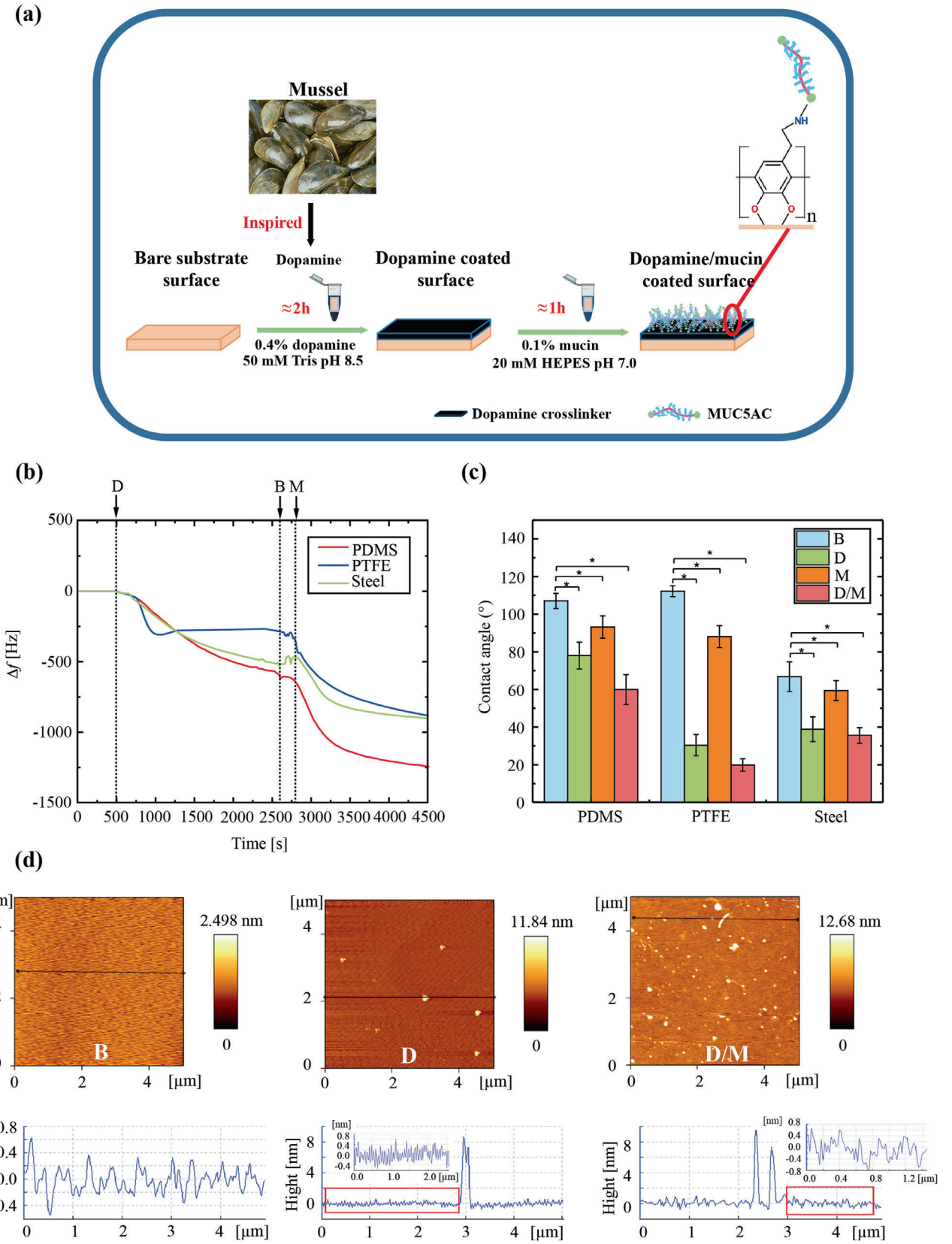

Figure 1. Preparation and characterization of dopamine/mucin double-layers generated by sequential adsorption. a) Samples were immersed into a 0.4% w/v dopamine solution for ≈2 h and then rinsed thoroughly with Millipore water to remove any unbound dopamine. After this dopamine pre-coating

we will test the correct formation of such a functional coating on exemplary medical devices.

2.2. Dopamine/Mucin Coatings Reduce Friction and Wear on PDMS

As we could demonstrate the successful formation of a dopamine/mucin double-layer on different substrates, we next evaluate the tribological properties of the coatings. We first analyze coatings generated on PDMS and use steel as a counterbody to probe the lubricity of the coating using a "poor" lubricant (i.e., simple HEPES buffer).[21] With this steel-on-PDMS material combination, one can mimic a hard-on-soft interface as present in several locations of the human body and, accordingly, this particular material combination is commonly used in biotribological studies.[23] Moreover, with this set of materials and the rotational tribology setup employed here, we can probe all three lubrication regimes (boundary, mixed, and hydrodynamic lubrication) in detail. To assess the influence of each molecular component used in the double-layer coatings on different lubrication modes, we not only analyze double-layer coatings, but also uncoated (bare) substrates and both, single dopamine and single mucin coatings.

As reported previously,[10f,21] the tribological properties of a steel-on-PDMS tribo-paring lubricated with simple buffer are very poor; the very high coefficient of friction (COF) μ we measure here in the boundary lubrication and mixed lubrication regime (**Figure 2**a) underscores this. In part, this bad tribological performance is due to the inability of hydrophobic PDMS to interact well with a water-based lubricant. As demonstrated by the contact angle measurements shown in Figure 1b, a dopamine coating renders a hydrophobic PDMS hydrophilic. Yet, this improvement in PDMS wettability alone is not very efficient in reducing friction: here, only the threshold between mixed lubrication and hydrodynamic lubrication is slightly shifted (Figure 2a). This effect is somewhat stronger for the single mucin coating; however, also here, friction in the boundary lubrication regime is still very high. Only for the double-layer coatings, the COF measured in the boundary lubrication is lowered significantly: here, μ is reduced by about one order of magnitude, and this represents decent lubricity suitable for biomedical applications.

In addition to the COF, we also evaluate wear formation on coated and uncoated PDMS. Considering the low wear rate of PDMS in short-time tribological tests, we here use the sensitive 3D surface roughness parameter, *Sq*, to compare the post-test surface to untreated samples and to quantify any occurring surface damage.[10f,24] As displayed in Figure 2b, an uncoated PDMS sample exhibits an ultra-low *Sq* value before exposure to tribological stress, and this low *Sq* value indicates a very smooth surface texture. After coating with any of the biomolecules tested here, this roughness parameter is increased by approximately one order of magnitude. With this increased surface roughness, one could expect that the coated surfaces are more prone to wear formation than the uncoated PDMS samples. However, we observe the opposite behavior: Without a protective coating, the *Sq* value of a PDMS surface is increased by a factor of ≈10, which indeed indicates wear formation; in contrast, with any of the tested coatings, such a pronounced increase in the sample roughness does not occur after tribological treatment.

In a next step, we ask if the dopamine/mucin coatings remain functional after a mechanical challenge. For this purpose, we conduct tribological tests with dopamine/mucin coatings using a higher (but constant) sliding velocity of 12 mm s^{-1} and an extended exposure time to tribo-stress of 1 h.[25] Interestingly, with this set of parameters, we obtain a nearly constant COF over time (Figure 2c), and the measured value of $\mu < 0.01$ agrees very well with the results shown in Figure 2a. This indicates that, although the detailed binding mechanism of dopamine to different materials is not fully understood, the stability of the double-layer coatings is very good. Of course, when applied to a medical device inserted into the human body, the dopamine/mucin double-layer will also be challenged by continuous contact with liquid, and this might induce hydrolysis of the biomolecule coating. Thus, we mimic this physiological challenge by incubating a sample set coated with a dopamine/mucin double-layer in a DPBS solution (pH 7.4) for 7 days at RT and comparing the tribological performance of this incubated sample set to samples carrying freshly prepared double-layer coatings. Importantly, both the freshly prepared and the incubated sample set show virtually identical lubricity (Figure 2c,d) in speed-dependent and in time-dependent friction tests. This result is underscored by light microscopy experiments where similar amounts of fluorescently labeled mucins are detected after different incubation times in the DPBS solution (Figure S1, Supporting Information).

Together, these experiments allow us to conclude that the dopamine-assisted immobilization of mucin on PDMS creates a double-layer that reduces both, friction and wear, and is stable toward mechanical challenge and storage in aqueous environments.

2.3. Dopamine/Mucin Coatings Prevent Surface Colonization by Eukaryotic Cells

A key property of dopamine we use here is its ability to create a sticky layer on a substrate, and we can generate dopamine pre-coatings on different inorganic materials, which are typically used in biomedical engineering. However, a sticky surface on medical devices can promote surface colonization with cells which, in turn, can induce thrombus formations and inflammatory responses.[26] Mucin coatings generated by simple passive

step, the samples were dipped into a 0.1% w/v mucin solution for ≈1 h, and then thoroughly rinsed again with Millipore water. b) Changes in frequency shift (Δf) are shown as they occur after sequential exposure of the sensor chips to a dopamine solution followed by rinsing with a mucin solution. The results denote the average as obtained from $n = 2$ independent measurements. c) Contact angle measurements were conducted on PDMS, PTFE, and steel surfaces. Samples were characterized in their bare state (B) as well as when carrying either a dopamine (D), mucin (M), or dopamine/mucin (D/M) coatings. The error bars denote the standard deviation as obtained from $n = 6$ independent measurements. Asterisks (*) indicate statistical significance using a p value of 0.05. d) Representative AFM images and cross-sectional profiles of mica substrates in their bare state (B) and when carrying a dopamine (D) or dopamine/mucin (D/M) coatings. The black lines in the AFM images denote the location where the cross-sectional profiles have been determined.

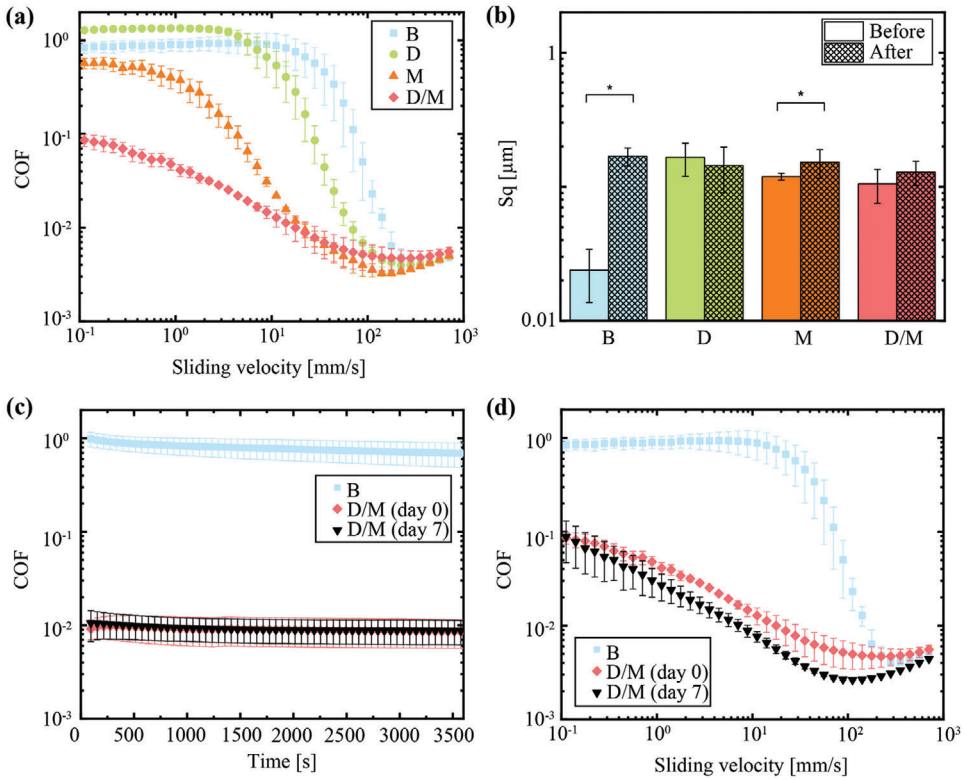

Figure 2. Tribological properties of dopamine/mucin coatings generated on PDMS. All data shown in this figure was obtained on a steel (ball)-on-PDMS (pins) material pairing using a 20 mM HEPES buffer (pH 7) as a lubricant. a) Stribeck curves as obtained for bare (B) PDMS samples or samples carrying a dopamine (D), mucin (M), or dopamine/mucin (D/M) coatings. b) Surface roughness (*Sq*) of PMDS surfaces carrying different coatings. Values obtained before and after a speed-dependent tribological test are compared. Asterisks (*) indicate statistically significant differences based on a p value of 0.05. c) Friction response of bare (B) and dopamine/mucin (D/M) coated samples at a constant sliding velocity of 12 mm s^{-1} and d) as a function of the sliding speed. For coated samples, results obtained with freshly prepared (day 0) and stored samples (day 7) are compared. All error bars denote the standard deviation as obtained from $n = 3$ independent measurements.

adsorption have already been shown to reduce this biofouling problem, but they are not stable enough to provide this property in an application where they are exposed to shear forces. Thus, in a next step, we ask if our stable dopamine/mucin double-layer coatings exhibit suitable anti-biofouling properties.

Yet, before we generate the coating on real medical devices, pilot experiments are conducted on a cell-binding surface of a 96 microtiter well plate. With this model surface, we test for putative cytotoxic effects in the presence and absence of the dopamine/mucin coating; we conduct incubation tests with two eukaryotic cell types to ensure that the double-layer coatings we generate indeed provide anti-adhesive properties and reduce unwanted cell colonization (see , Section 4 for details). We assess the cell-repellent properties of the dopamine/mucin double-layer by comparing the colonization of commercial tissue culture substrates by fibroblasts (**Figure 3**a) and epithelial cells (Figure 3b). Indeed, as expected, we find that the double-layer coatings reduce cellular attachment by ≈90% for fibroblasts and by ≈95% for epithelial cells. In addition, fluorescence images obtained for both cell lines show an altered morphology for the samples carrying the double-layer coatings: here, we find mostly cells with round shapes indicating weak adhesion; in contrast, on the uncoated samples, both cell types assume a well-spread, extended morphology as typical for strongly adherent cells. Results from a viability staining verify that dopamine/mucin-layer is indeed only cell-repellent, but not cytotoxic (Figure S2, Supporting Information). Importantly, on control samples carrying a dopamine coating only, we find a similarly high number of fibroblast cells as on the uncoated samples, and somewhat reduced but still high numbers of epithelial cells. Together with the results obtained from the friction tests discussed above (see Section 2.2.), this shows that a dopamine coating alone is not suitable for an application on medical devices. Thus, further experiments are only conducted with the dopamine/mucin double-layers.

2.4. Dopamine/Mucin Coatings Reduce Wear at High Contact Pressure

So far, we have analyzed the tribological properties of dopamine/mucin coatings on PDMS, a material which is rather resistant to wear formation. In a next step, we ask if dopamine/mucin coatings can also provide wear protection on more sensitive materials and at higher contact pressures. Thus, we next test the wear protection abilities of dopamine/mucin coatings on PTFE, a material that is highly prone to wear damage[27]—especially when probed with a hard counter material such as the steel sphere we use here. Since PTFE itself

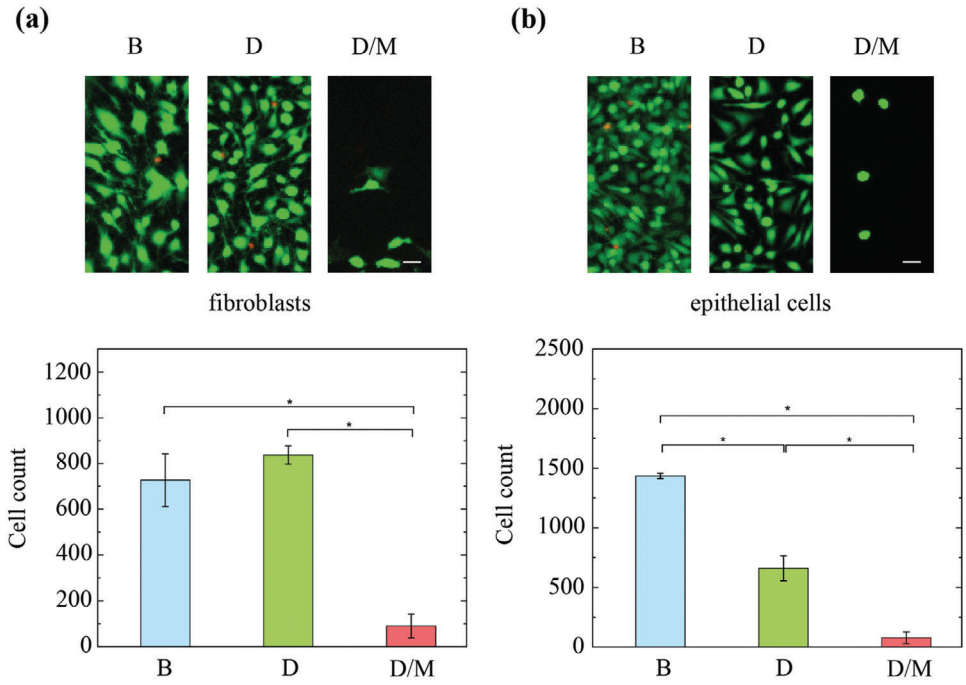

Figure 3. Cellular colonization of dopamine and dopamine/mucin coated surfaces. The attachment of a) fibroblasts and b) epithelial cells onto a cell-binding surface without any coating (B, control) as well as with a dopamine (D) and dopamine/mucin (D/M) coatings is compared. The scale bar represents 50 µm and applies to all six images. The error bars represent the standard error of the mean as obtained from analytical triplicates. Asterisks (*) indicate statistically significant differences based on a p value of 0.05.

acts as a solid lubricant,[28] the COFs obtained with this material pairing (**Figure 4**a) are lower than the ones obtained on PDMS. Interestingly, also on this substrate, the dopamine/mucin coatings improve the lubricity—albeit only slightly. After tribological testing, we evaluate the material surface using a 3D laser scanning microscope. Representative images of the obtained 3D topographies of both, bare and coated PTFE surfaces, are shown in Figure 4c,d: In both cases, there are some plowing grooves in the center of the wear feature and material pile-up at the edge. This indicates that severe abrasion and plastic deformation occurs during the tribological treatment.[29] However, as summarized in Figure 4b, a quantification of those similar images shows that the wear volume of dopamine/mucin coated PTFE samples is reduced by half compared to the uncoated samples. Consistently, also the diameter of the wear scar is reduced by the coating.

We rationalize this result as follows: First, with the assistance of dopamine, the mucin coating strongly decreases the contact angle of PTFE, shifting its surface properties from hydrophobic to hydrophilic thus improving its interaction with an aqueous lubricant. Moreover, the surface-bound layer of mucin molecules will provide hydration lubrication thus slightly reducing the COF even in the boundary lubrication regime. Furthermore, the macromolecular coating on the PTFE surface will also play a role in supporting/redistributing the applied load, restrict the removal of PTFE material from the surface and therefore protect the surface from severe wear damage.

Importantly, with this steel-on-PTFE material pairing and the measuring parameters chosen here, the resulting contact pressure (according to Hertzian theory) is ≈23 MPa. This is a similarly high level as what artificial joint prostheses experience under physiological load.[30] Thus, the dopamine/mucin coatings might even be able to reduce friction and wear formation in artificial joints. We test this idea by exploring another material combination, that is, coated steel probed with a polyetheretherketone (PEEK) counter body. This choice is motivated by three aspects: first, steel is a material which is widely used in biomedical applications but—compared to hydrophobic polymer materials—only allows for low levels of passive mucin adsorption[21]; second, PEEK is often employed as a counter material for biotribological tests[1d,8]; third, with this particular set of experiments, we aim to mimic highly challenging conditions in the boundary lubrication regime where a high contact pressure is expected to entail asperity-to-asperity contact and thus significant wear formation. In other words, the chances of the coating to provide protective properties are rather low. Indeed, the speed-dependent COFs obtained on bare and coated steel samples are very similar (**Figure 5**a), and we find clear wear features on both sample variants (Figure 5b,d). The most prominent wear morphology we detected is line-shaped features, which we attribute to abrasive wear caused by local inhomogeneities of the tribo-paring during every rotation. Overall, owing to the high hardness and elastic modulus of steel, the caused wear volume is approximately an order of magnitude lower than what we found for PTFE surfaces, and the wear diameter is smaller as well. Importantly, when those two wear parameters are compared for coated and uncoated samples, we find a small but significant reduction of both features for the dopamine/mucin coated samples. This result is astonishing given the harsh conditions the material pairing was subjected to. It does, however, underline the great potential the presented

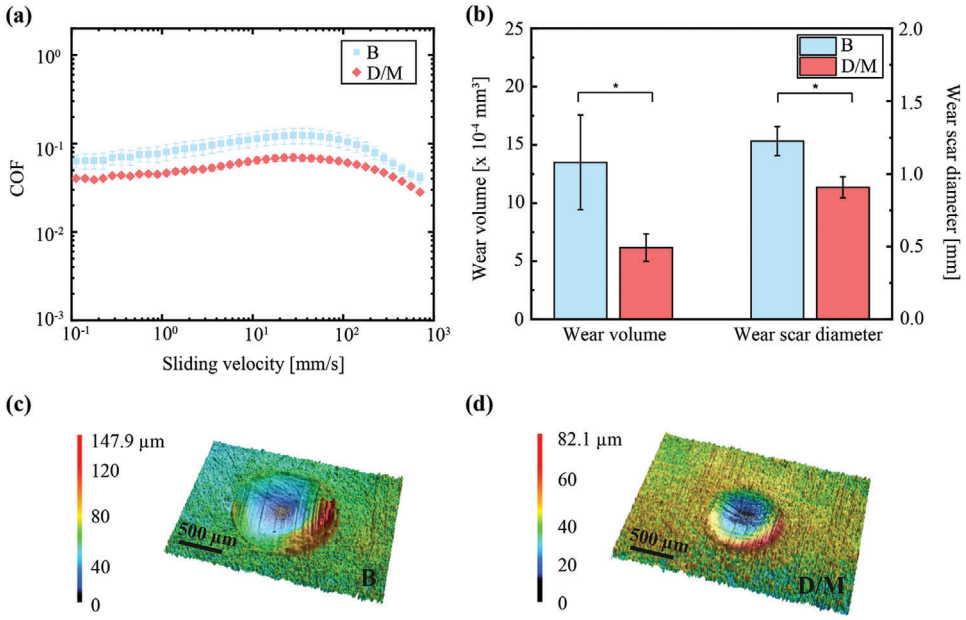

Figure 4. Tribological properties of dopamine/mucin coatings generated on PTFE. All data shown in this figure was obtained on a steel (ball)-on-PTFE (pins) material pairing using a 20 mM HEPES buffer (pH 7) as a lubricant. a) Stribeck curves as obtained for bare (B) PTFE samples or samples carrying dopamine/mucin (D/M) coatings. b) Wear volume and wear scar diameter of the PTFE surfaces as calculated after a tribological test. The error bars displayed above denote the standard deviation as obtained from a) $n = 3$ and b) $n = 9$ independent measurements, respectively. Asterisks (*) indicate statistically significant differences based on a p value of 0.05. c,d) depict example 3D images of a bare PTFE surface c) after tribological measurement as compared to a dopamine/mucin coated PTFE surface d). Please note the different z-scales in c) and d).

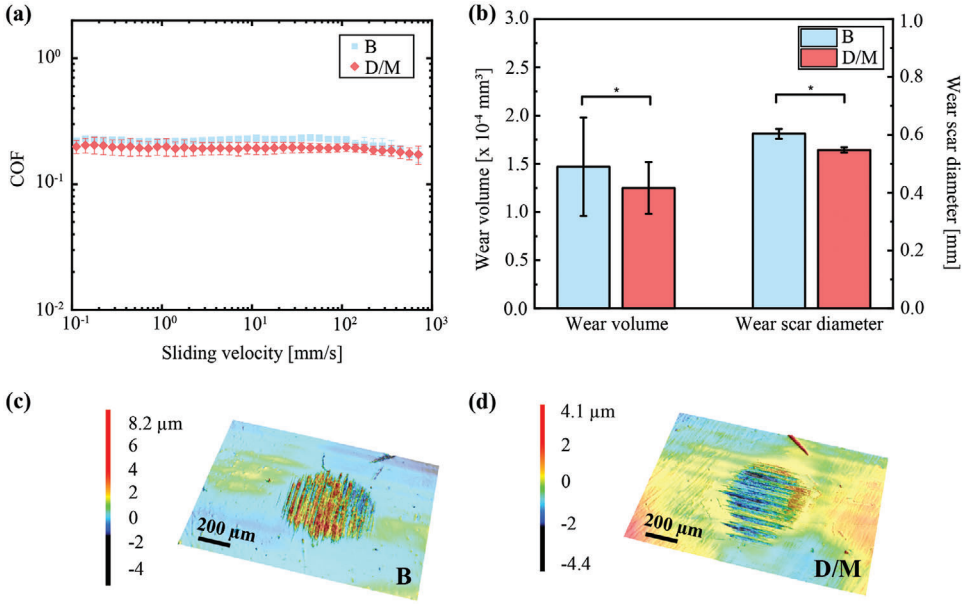

Figure 5. Tribological properties of dopamine/mucin coatings generated on steel surfaces. All data shown was obtained on a PEEK (ball)-on-steel (pins) material pairing using 20 mM HEPES buffer (pH 7) as a lubricant. a) Stribeck curves as obtained for bare (B) steel samples or samples carrying dopamine/mucin (D/M) coatings. b) Wear volume and wear scar diameter of the steel surfaces as calculated after a tribological test. The error bars displayed above denote the standard deviation as obtained from a) $n = 3$ and b) $n = 9$ independent measurements, respectively. Asterisks (*) indicate statistically significant differences based on a p value of 0.05. c,d) depict example 3D images of a bare steel surface c) after tribological measurement as compared to a dopamine/mucin coated steel surface d). Please note the different z-scales in c) and d).

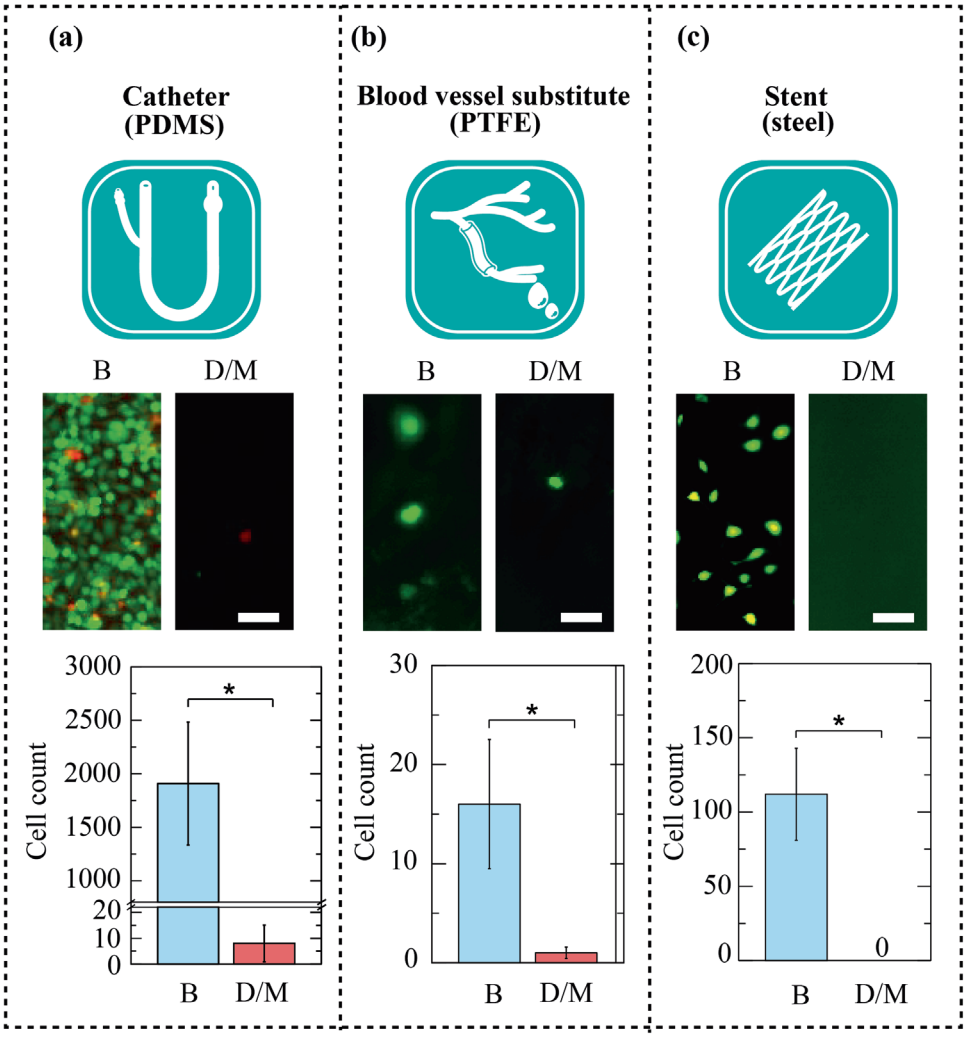

Figure 6. Epithelial cell colonization of commercial medical devices. The colonization efficiency of HeLa cells seeded onto untreated (B) and dopamine/mucin (D/M) coated catheter a), blood vessel substitute b), and stent c) samples are compared. The scale bar corresponds to 50 μm and applies to all fluorescence images. Error bars represent the standard error of the mean obtained from triplicates, and asterisks denote statistical significance ($p < 0.05$).

dopamine/mucin double-layer holds for protecting an underlying substrate.

2.5. Dopamine/Mucin Coatings Establish Cell-Repellent Surfaces on Medical Devices

Having demonstrated that the dopamine/mucin double-layer coatings successfully cover PDMS, steel, and PTFE sample surfaces, provide lubricity and reduce wear formation on all those materials, we now, in a final step, ask if such coatings can also form protective layers on real medical devices made from those materials. The three examples of medical devices we generate our double-layer coatings on are steel-based stents, PDMS-based catheters, and PTFE-based blood vessel substitutes. Since tribology measurements are very difficult to perform with both, highly curved samples such as catheters and fragile objects such as stents, we use cell colonization experiments to assess the functionality of the dopamine/mucin coated device surfaces in comparison to their uncoated counterparts. Indeed, as the three devices we test here can all trigger restenosis in vivo, a cell-repellent surface is an important feature for each of them. As a cell line for those experiments, we select epithelial HeLa cells, which are easy to handle and frequently used as model cells in studies characterizing the biocompatibility of both, metallic- and PTFE-based materials.[31]

As depicted in **Figure 6** and Figure S3, Supporting Information, the three (uncoated) medical devices are colonized by HeLa cells with very different efficiencies: We find the highest density of HeLa cells on the PDMS-based catheter sample and the lowest density on the PTFE-based blood vessel substitute. Indeed, the low number of round cells we detect on blood vessel substitute and stent samples suggests that, here, the cells only weakly interact with the material.[32] This could indicate that the manufacturers of the three devices might already have applied some type of surface treatment to reduce the cell-adhesive properties of their

products. Yet, even if such a surface treatment has not been conducted, those findings agree well with previous results from the literature which have reported good cell adhesion on PDMS as well as cell-repellent properties for PTFE.[12,33] Anyways, based on the results discussed above (see Section 2.3.), it is possible that a reduction in the cell colonization efficiency can be achieved with our double-layer coatings for all three devices—even for the PTFE-based blood vessel substitute. Indeed, this is what we find: in all three cases, the dopamine/mucin coatings reduce cellular attachment by more than 90%. Together, this shows that all three commercial medical products benefit from our coating and it suggests that the coating could help to reduce adverse reactions such as neointimal proliferation or adhesions. At the same time, it suggests that other anti-biofouling properties reported earlier for passively adsorbed mucin layers or covalent mucin coatings (such as a reduction of bacterial adhesion or protein adsorption) should be provided by the dopamine/mucin coatings as well.[12,34] Of course, when applied in a physiological setting, those three devices will encounter site-specific challenges that could affect the functionality of the dopamine/mucin coatings. Thus, it will be a necessary next step in future research to assess the long-term stability and functionality of dopamine/mucin coatings under realistic conditions in vivo.

3. Conclusion

Inspired by the adhesion of mussels, we here develop dopamine/mucin coatings using a simple two-step dip-coating approach. With this strategy, we introduce an easy and bio-based method to form non-covalent but stable mucin coatings onto both, flat commercial materials and real medical devices alike. Typically, with conventional coating processes, it is very difficult to generate a stable coating on PTFE or steel surfaces.[35] With the approach we developed in this study, however, mucin-based coatings are easily possible on PTFE-based blood vessel substitutes and steel-based stents. Our results demonstrate that the dopamine-assisted immobilization of mucin creates a molecular double-layer that decreases friction (especially in the boundary lubrication regime), reduces surface damage, and provides cell-repellent properties. Since dopamine can firmly bind to almost every surface, the double-layer coatings we characterized here have great potential to be applied to other medical devices as well: metal-based artificial heart valves, ceramic-based artificial joints, and polymer-based ocular prostheses, for instance, would benefit from surfaces with low friction, good wear protection, and anti-biofouling properties.

4. Experimental Section

Aqueous Solutions: HEPES buffer and Tris buffer were prepared by dissolving either 20 mM 4-(2-hydroxyethyl)-1-piperazineethanesulfonic acid (HN78.2, Roth, Karlsruhe, Germany) or 50 mM Tris-(hydroxymethyl)aminomethane (A1379, AppliChem, Darmstadt, Germany) in Millipore water. The final pH values of the HEPES buffer (pH 7.0) and Tris buffer (pH 8.5) solutions used here were adjusted with NaOH or HCl as needed. Solutions containing in-lab purified porcine gastric mucin (see Supporting Information for details of the purification process) were generated at a concentration of 0.1% w/v (=1 mg mL^{-1}) in HEPES buffer by incubating lyophilized mucin in HEPES buffer at room temperature overnight.[10f] Dopamine hydrochloride (H8502, Sigma, St. Louis, MO, USA) was dissolved at a concentration of 0.4% w/v (=4 mg mL^{-1}) in Tris buffer to obtain the polydopamine solution for the coating process described below.[36]

Coating Process: To investigate the functionality and stability of the dopamine/mucin coatings described here, cylinders made of PDMS, PTFE, or stainless steel were used (see Supporting Information for details). The coatings were prepared by first depositing a dopamine layer on the substrate surface using a dip-coating method (Figure 1a). In detail, the steel, PDMS, or PTFE substrates were immersed into the dopamine solution for ≈2 h and then thoroughly rinsed with Millipore water to remove any unbound dopamine. Afterward, the dopamine pre-coated substrates were placed into the mucin solution, incubated for ≈1 h, and then again thoroughly rinsed with Millipore water. Single dopamine coatings or single mucin coatings were developed for comparison by performing only one incubation step each.

QCM-D Measurements: To confirm that the envisioned dopamine/mucin coatings are indeed generated on the substrates tested here, the adsorption behavior of dopamine and mucin on different substrates was studied using a QCM-D with a qcell T-Q2 platform (3T-Analytik, Tuttlingen, Germany). For those microscopic adsorption tests, quartz chips with stainless steel, PTFE, and PMDS surfaces were selected (see Supporting Information for details) to ensure comparability to the tests conducted with macroscopic dopamine/mucin coatings. With those different chips, adsorption experiments were conducted as follows: at the beginning of each adsorption test, a pure buffer solution (devoid of dopamine and mucin) was injected at a flow rate of 100 µL min^{-1} until a stable baseline was obtained. Then, a dopamine solution was injected at a rate of 100 µL min^{-1} for ≈30 min and the change in frequency shift (Δf, Hz) as automatically calculated by the software "qGraph" (3T-Analytik, Tuttlingen, Germany) was recorded. After rinsing with a pure buffer solution (flow rate: 1000 µL min^{-1}) for ≈2 min, a mucin solution was injected at 100 µL min^{-1} for ≈30 min to obtain an adsorption curve.

Cell Cultivation and Surface Colonization Experiments: Human epithelial cells (HeLa) were cultured using Minimum Essential Medium Eagle (MEM, M2279, Sigma) supplemented with 10% v/v fetal bovine serum (FBS, F9665, Sigma), a 2 mM L-glutamine solution (Sigma), a 1% v/v non-essential amino acid solution (NEAA, M7145 Sigma), and 1% v/v penicillin/streptomycin (76437, Sigma). Human fibroblast cells (NIH-3T3) were cultured with Dulbecco's Modified Eagle's high glucose Medium (DMEM, D5796, Sigma) supplemented with 10% v/v FBS and 1% v/v penicillin/streptomycin. For both cell types, the environment was adjusted to 37 °C and 5% CO_2 in a humidified atmosphere.

For surface colonization and viability tests, 12 wells of a 96-well plate (M0812-100EA, Sigma) were prepared for each cell type; here, three wells were coated with dopamine and three were coated with dopamine/mucin double-layers as described in Section 2.2. The remaining six wells were left untreated for positive and negative controls. Afterward, all wells were washed three times with sterile Dulbecco's Phosphate Buffered Saline (DPBS, 882104, Sigma). Subsequently, the HeLa and NIH-3T3 cells were seeded into the wells at a concentration of 30 000 cells per well and cultivated in 200 µL medium for 24 h. As a control inducing low cell viability, methanol (MeOH, 4627.1, Roth) was added to a final concentration of 50% v/v 4 h before starting the live/dead analysis. For live/dead staining, the cells were washed with DPBS and 200 µL of DPBS supplemented with 1 µM calcein AM (Invitrogen, Carlsbad, CA, USA) and 2 µM ethidium homodimer 1 (Invitrogen) were added to each well. After 30 min of incubation, fluorescence images of living cells (green color) and dead cells (red color) were recorded using the DMi8 microscope (Leica, Wetzlar, Germany) equipped with a 10x objective (Leica) and a digital camera (Orca Flash 4.0 C11440-22C, Hamamatsu, Japan).

Very similar cell colonization experiments were conducted with HeLa cells seeded onto commercial medical devices: stent (steel, AS-21XXL, Andramed, Reutlingen, Germany), blood vessel substitute (PTFE, Steris, USA), and catheter (PDMS, U400, Medi1one Medical, Fellbech, Germany) samples were coated with a dopamine/mucin double-layer. The cell-repellent properties of the dopamine/mucin coatings were assessed with fluorescence microscopy as described above.

Tribological Tests: The tribological experiments were performed at 21 °C using the rotational tribology unit (T-PTD 200, Anton Paar, Graz, Austria) of a commercial shear rheometer (MCR 302, Anton Paar) as described before.[37] The tribological properties, that is, lubricity and wear resistance, of the coatings were evaluated on different substrates. As counter-parts for these tribological tests, commercial spheres made from either stainless steel (1.4404, Kugel Pompel, Vienna, Austria) or PEEK (Victrex 450G, Yuwei, Nanjing, China) with a diameter of 12.7 mm were used as received. Further polishing was not necessary as both sphere types showed low roughness (i.e., $Sq_{steel} < 200$ nm, $Sq_{PEEK} < 500$ nm) when analyzed with a laser scanning microscope (VK-X1100, Keyence, Osaka, Japan). The lower samples in the tribological measuring configuration carried the coatings were mounted into a sample holder, and coatings were generated in situ. Then, the coated samples were first washed with ultrapure water before 600 µL of a lubricant solution was applied onto the three pions to ensure full coverage with liquid. For measurements, the normal load was chosen to be 6 N. With this load, the average contact pressure can be estimated based on Hertz contact theory with the following equations:

$$p = \frac{2}{3}p_{max} = \frac{2}{3\pi} \cdot \sqrt[3]{\frac{6 \cdot f_{n.per\,pin} \cdot E'^2}{R^2}} \quad (1)$$

$$\frac{1}{E'} = \frac{1-\nu_1^2}{E_1} + \frac{1-\nu_2^2}{E_2} \quad (2)$$

with the Young's moduli and Poisson's ratios displayed in Table S1, Supporting Information. With this approach, an average contact pressure of ≈0.3 MPa for the steel-on-PDMS pairing, ≈23 MPa for steel-on-PTFE pairing, and ≈44 MPa for the PEEK-on-steel pairing was obtained. To explore as many lubrication regimes as possible, the sliding velocity was varied from 10^{-1} to 10^3 mm s^{-1}. For each condition, three independent experiments were carried out using a fresh set of pins for each measurement.

The durability of the dopamine/mucin coatings were evaluated on PDMS samples as follows: First, dopamine/mucin coated samples were exposed to UV-light for 1 h for sterilization[21] and then stored in a commercial DPBS solution (pH 7.4, Lonza, Verviers, Belgium) at room temperature for 7 days. Those storage conditions were chosen to mimic conditions that implanted materials/medical devices experience within the human body. Afterward, the tribological properties were probed using the same tribology unit as above using steel spheres as counter bodies. Here, the sliding velocity was first varied from 10^{-1} to 10^3 mm s^{-1} and then set to a constant value of 12 mm s^{-1} for 1 h.

Surface Characterization: The wetting behavior of the coated samples was evaluated by calculating the static contact angle (CA). In brief, a 10 µL drop of Millipore water was pipetted onto the sample surface, and a transversal image of the liquid–solid interface was acquired using a high-resolution camera (Point Gray Research, Richmond, Canada). Then, the CA was determined using the drop-snake analysis tool, a plug-in for the software "ImageJ" (v 1.8.0, NIH, Bethesda, MD, USA). For each condition, at least three independent measurements were carried out.

The surface topography of the samples was investigated using a 3D laser scanning microscope (VK-X1100, Keyence, Osaka, Japan). From the obtained topographical images, the surface roughness, *Sq* (root mean square height) was calculated using the software "MultiFile Analyzer" (Keyence, Osaka, Japan). Owing to the ultralow wear rate of PDMS in short-time tribological lab experiments,[10f] only the wear rates (wear volume and diameter of wear scar) of PTFE and steel samples were evaluated.

The morphological characterization of the samples at the nanoscale was performed using a NanoWizard II atomic force microscope (AFM, JPK Instruments, Berlin, Germany). Samples were probed in air using an OMCL-AC160TS-R3 cantilever (Olympus, Tokyo, Japan). Before imaging, the AFM was allowed to thermally equilibrate for 30 min. A 20 µL drop of the tested sample solution was pipetted onto a freshly cleaved mica slide (dimensions: 1 mm × 1 mm), incubated for 10 min, then rinsed with Millipore water and finally dried with compressed nitrogen gas. Images were acquired in tapping mode at room temperature over an area of 5 µm × 5 µm. From the obtained topographical images, representative cross-sectional profiles were analyzed using the SPM Image Processing software (v.3.3.20, JPK).

Statistical Analysis: To evaluate the significant differences between two samples, independent two-sample *t*-test was performed.[12] Prior to statistical analysis, the normal distribution of the results was verified with the Shapiro–Wilk test, and the homogeneity of variances was measured using the F-test. For non-normal distributed variances, the Wilcoxon–Mann–Whitney-test was used. Student's *t*-tests were applied for normal distributed homogenous variances, whereas a Welch's *t*-test was performed for unequal variances. The software "Origin" (OriginPro 2020, OriginLab Corp., Northampton, MA, USA) was used to conduct all statistical tests. For *p*-values <0.05, differences were considered to be statistically significant, and significant differences between tested groups are marked with an asterisk in all graphs.

Supporting Information

Supporting Information is available from the Wiley Online Library or from the author.

Acknowledgements

The authors thank Matthias Marczynski for assistance with the mucin purification and Benjamin Winkeljann for help regarding the sample preparation. This project received funding from the European Union's Horizon 2020 research and innovation programme under the Marie Skłodowska-Curie Grant Agreement No 754462.

Open access funding enabled and organized by Projekt DEAL.

Conflict of Interest

The authors declare no conflict of interest.

Author Contributions

J.S. and T.M.L. contributed equally to this work. J.S. and O.L. designed the study, J.S. and T.M.L. performed the experiments and analyzed data. N.L. contributed medical materials. All authors contributed to the discussion of the data, wrote the manuscript, and gave approval to the final version of the manuscript.

Keywords

anti-biofouling, friction, implants, molecular double-layers, wear protection

Received: May 16, 2020
Revised: August 9, 2020
Published online:

[1] a) C. R. Arciola, D. Campoccia, L. Montanaro, *Nat. Rev. Microbiol.* **2018**, *16*, 397; b) J. Song, Z. Liao, H. Shi, D. Xiang, Y. Liu, W. Liu, Z. Peng, *Tribol. Lett.* **2017**, *65*, 150; c) A. J. T. Teo, A. Mishra, I. Park, Y.-J. Kim, W.-T. Park, Y.-J. Yoon, *ACS Biomater. Sci. Eng.* **2016**, *2*, 454; d) S. M. Kurtz, J. N. Devine, *Biomaterials* **2007**, *28*, 4845; e) A. Girotti, D. Orbanic, A. Ibáñez-Fonseca, C. Gonzalez-Obeso, J. C. Rodríguez-Cabello, *Adv. Healthcare Mater.* **2015**, *4*, 2423.

[2] A. M. Hussein, S. A. Mohammed, N. Al-Aqeeli, *Materials* **2015**, *8*, 2749.
[3] a) J. L. Harding, M. M. Reynolds, *Trends Biotechnol.* **2014**, *32*, 140; b) B. Cao, Q. Tang, L. Li, J. Humble, H. Wu, L. Liu, G. Cheng, *Adv. Healthcare Mater.* **2013**, *2*, 1096.
[4] a) R. A. Byrne, M. Joner, F. Alfonso, A. Kastrati, *Nat. Rev. Cardiol.* **2014**, *11*, 13; b) P. Roy-Chaudhury, B. S. Kelly, M. A. Miller, A. Reaves, J. Armstrong, N. Nanayakkara, S. C. Heffelfinger, *Kidney Int.* **2001**, *59*, 2325.
[5] D. Buccheri, D. Piraino, G. Andolina, B. Cortese, *J. Thorac. Dis.* **2016**, *8*, E1150.
[6] C. P. McCoy, N. J. Irwin, L. Donnelly, D. S. Jones, J. G. Hardy, L. Carson, *Int. J. Pharm.* **2018**, *535*, 420.
[7] M. T. Barford Jessica, Y. Hu, K. Anson, R. M. Coates Anthony, *J. Urol.* **2008**, *180*, 1522.
[8] J. Song, Y. Liu, Z. Liao, S. Wang, R. Tyagi, W. Liu, *Mater. Sci. Eng., C* **2016**, *69*, 985.
[9] V. Yesilyurt, O. Veiseh, J. C. Doloff, J. Li, S. Bose, X. Xie, A. R. Bader, M. Chen, M. J. Webber, A. J. Vegas, R. Langer, D. G. Anderson, *Adv. Healthcare Mater.* **2017**, *6*, 1601091.
[10] a) J. M. Coles, D. P. Chang, S. Zauscher, *Curr. Opin. Colloid Interface Sci.* **2010**, *15*, 406; b) O. Svensson, T. Arnebrant, *Curr. Opin. Colloid Interface Sci.* **2010**, *15*, 395; c) B. Winkeljann, K. Boettcher, B. N. Balzer, O. Lieleg, *Adv. Mater. Interfaces* **2017**, *4*, 1700186; d) T. Sandberg, M. Karlsson Ott, J. Carlsson, A. Feiler, K. D. Caldwell, *J. Biomed. Mater. Res., Part A* **2009**, *91A*, 773; e) N. Nikogeorgos, P. Efler, A. B. Kayitmazer, S. Lee, *Soft Matter* **2015**, *11*, 489; f) B. Winkeljann, P.-M. A. Leipold, O. Lieleg, *Adv. Mater. Interfaces* **2019**, *6*, 1900366; g) S. K. Linden, P. Sutton, N. G. Karlsson, V. Korolik, M. A. McGuckin, *Mucosal Immunol.* **2008**, *1*, 183.
[11] a) R. R. R. Janairo, Y. Zhu, T. Chen, S. Li, *Tissue Eng., Part A* **2013**, *20*, 285; b) I. A. Bushnak, F. H. Labeed, R. P. Sear, J. L. Keddie, *Biofouling* **2010**, *26*, 387.
[12] B. Winkeljann, M. G. Bauer, M. Marczynski, T. Rauh, S. A. Sieber, O. Lieleg, *Adv. Mater. Interfaces* **2020**, *7*, 1902069.
[13] a) E. Faure, P. Lecomte, S. Lenoir, C. Vreuls, C. Van De Weerdt, C. Archambeau, J. Martial, C. Jérôme, A.-S. Duwez, C. Detrembleur, *J. Mater. Chem.* **2011**, *21*, 7901; b) S. Kruss, T. Wolfram, R. Martin, S. Neubauer, H. Kessler, J. P. Spatz, *Adv. Mater.* **2010**, *22*, 5499.
[14] H. Lee, S. M. Dellatore, W. M. Miller, P. B. Messersmith, *Science* **2007**, *318*, 426.
[15] W.-Z. Qiu, H.-C. Yang, Z.-K. Xu, *Adv. Colloid Interface Sci.* **2018**, *256*, 111.
[16] Y. Liu, C.-P. Chang, T. Sun, *Langmuir* **2014**, *30*, 3118.
[17] Y. Zhang, B. Thingholm, K. N. Goldie, R. Ogaki, B. Städler, *Langmuir* **2012**, *28*, 17585.
[18] Q. Fu, X. Li, Q. Zhang, F. Yang, W. Wei, Z. Xia, *J. Chromatogr. A* **2015**, *1416*, 94.
[19] R. Huang, X. Liu, H. Ye, R. Su, W. Qi, L. Wang, Z. He, *Langmuir* **2015**, *31*, 12061.
[20] a) N. S. Manam, W. S. W. Harun, D. N. A. Shri, S. A. C. Ghani, T. Kurniawan, M. H. Ismail, M. H. I. Ibrahim, *J. Alloys Compd.* **2017**, *701*, 698; b) M. M. M. Bilek, *Appl. Surf. Sci.* **2014**, *310*, 3; c) C. Diaz Blanco, A. Ortner, R. Dimitrov, A. Navarro, E. Mendoza, T. Tzanov, *ACS Appl. Mater. Interfaces* **2014**, *6*, 11385; d) C. Kimna, B. Winkeljann, J. Song, O. Lieleg, *Adv. Mater. Interfaces* **2020**, 202000735, unpublished, https://doi.org/10.1002/admi.202000735.
[21] J. Song, B. Winkeljann, O. Lieleg, *ACS Appl. Bio Mater.* **2019**, *2*, 3448.
[22] M. Marczynski, B. N. Balzer, K. Jiang, T. M. Lutz, T. Crouzier, O. Lieleg, *Colloids Surf., B* **2020**, *187*, 110614.
[23] A. Sarkar, E. M. Krop, *Curr. Opin. Food Sci.* **2019**, *27*, 64.
[24] K. Boettcher, B. Winkeljann, T. A. Schmidt, O. Lieleg, *Biotribology* **2017**, *12*, 43.
[25] J. Song, Z. Liao, S. Wang, Y. Liu, W. Liu, R. Tyagi, *J. Mater. Eng. Perform.* **2016**, *25*, 116.
[26] T. Goda, T. Konno, M. Takai, K. Ishihara, *Colloids Surf., B* **2007**, *54*, 67.
[27] S. Affatato, A. Ruggiero, M. Merola, *Composites, Part B* **2015**, *83*, 276.
[28] T. W. Scharf, S. V. Prasad, *J. Mater. Sci.* **2013**, *48*, 511.
[29] J. Song, H. Shi, Z. Liao, S. Wang, Y. Liu, W. Liu, Z. Peng, *Polymers* **2018**, *10*, 142.
[30] G. Lewis, *Bio-Med. Mater. Eng.* **1998**, *8*, 91.
[31] a) K. C. Chaw, M. Manimaran, F. E. H. Tay, S. Swaminathan, *Microvasc. Res.* **2006**, *72*, 153; b) B. Joddar, A. Albayrak, J. Kang, M. Nishihara, H. Abe, Y. Ito, *Acta Biomater.* **2013**, *9*, 6753.
[32] T. Crouzier, H. Jang, J. Ahn, R. Stocker, K. Ribbeck, *Biomacromolecules* **2013**, *14*, 3010.
[33] a) B. J. Klenkler, D. Dwivedi, J. A. West-Mays, H. Sheardown, *J. Biomed. Mater. Res., Part A* **2010**, *93A*, 1043; b) R. Sipehia, G. Martucci, M. Barbarosie, C. Wu, *Biomater., Artif. Cells, Immobilization Biotechnol.* **1993**, *21*, 455; c) M. Crombez, P. Chevallier, R. C. Gaudreault, E. Petitclerc, D. Mantovani, G. Laroche, *Biomaterials* **2005**, *26*, 7402.
[34] G. Petrou, T. Crouzier, *Biomater. Sci.* **2018**, *6*, 2282.
[35] J. Song, B. Winkeljann, O. Lieleg, *Adv. Mater. Interfaces* **2020**, 2000850, unpublished, https://doi.org/10.1002/admi.202000850
[36] a) S. Kasemset, A. Lee, D. J. Miller, B. D. Freeman, M. M. Sharma, *J. Membr. Sci.* **2013**, *425–426*, 208; b) F. Ponzio, P. Payamyar, A. Schneider, M. Winterhalter, J. Bour, F. Addiego, M.-P. Krafft, J. Hemmerle, V. Ball, *J. Phys. Chem. Lett.* **2014**, *5*, 3436.
[37] K. Boettcher, S. Grumbein, U. Winkler, J. Nachtsheim, O. Lieleg, *Rev. Sci. Instrum.* **2014**, *85*, 093903.